

The Impact of Metal-free Solar Reflective Film on Vehicle Climate Control

John P. Rugh and Robert B. Farrington
National Renewable Energy Laboratory

Jeffrey A. Boettcher
3M Automotive Division

Copyright © 2001 Society of Automotive Engineers, Inc.

ABSTRACT

The air-conditioning system can significantly impact the fuel economy and tailpipe emissions of automobiles. If the peak soak temperature of the passenger compartment can be reduced, the air-conditioner compressor can potentially be downsized while maintaining human thermal comfort. Solar reflective film is one way to reduce the peak soak temperature by reducing the solar heat gain into the passenger compartment. A 3M non-metallic solar reflective film (SRF) was tested in two minivans and two sport utility vehicles (SUV). The peak soak temperature was reduced resulting in a quicker cooldown. Using these data, a reduction in air-conditioner size was estimated and the fuel economy and tailpipe emissions were predicted.

INTRODUCTION

When operating, the air-conditioning compressor is the largest auxiliary load on today's automobile engines and significantly impacts fuel economy and tailpipe emissions. In addition to providing passenger comfort, the air-conditioning system performs a vital safety function in the form of dehumidifying the passenger compartment air to minimize condensation on the glazing surfaces. It is estimated that air conditioning in light duty vehicles in the United States increases annual gasoline consumption by 11 billion gallons¹ or nearly \$16 billion each year. Also, the automotive industry is facing the implementation of the new Supplemental Federal Test Procedure²(SFTP). The SFTP consists of the three tests shown in Table 1: the current Federal Test Procedure (FTP), an air-conditioning test (SC03), and a high-speed test (US06).

Table 1. Supplemental Federal Test Procedure Specifications

	FTP	SC03	US06
Time(s)	1877	594	600
Max. speed, km/h (mph)	91.2 (56.7)	88.2 (54.8)	129.2 (80.3)
Max. acceleration, km/h/s (mph/s)	5.8 (3.6)	8.2 (5.1)	12.9 (8)
Distance, km (miles)	17.8 (11.1)	5.8 (3.6)	12.9 (8)
Contribution to total emissions value	35%	37%	28%

The SC03 test will measure the tailpipe emissions of vehicles with the air conditioner operating at maximum fan speed, 100% recirculation, 100 grains of moisture/lb. of dry air, and 850 W/m² of solar radiation over a drive cycle of approximately 10 minutes. Use of the air conditioner increases NO_x by about 80%, CO by about 70%, and reduces fuel economy by about 20%.³

The air-conditioning system is sized to provide adequate cooling in a specified time period from a hot soak condition. Hence, one way to reduce air-conditioning fuel use is to reduce the peak soak temperatures in a vehicle. Solar reflective glazing ranks high among the various technologies to reduce the peak soak temperature.⁴ This paper discusses the testing and modeling results of a polymeric-based solar reflective film (SRF) developed for use in automotive glazing.

DESCRIPTION OF SOLAR REFLECTIVE FILM

The 3M SRF is a non-metallic and colorless film, which reflects infrared energy with a high visible light transmission. The 100% polymeric film does not corrode and attenuate electromagnetic transmission/reception from cell phones and other communication devices. These features enable design flexibility in the overall glazing construction.

VEHICLE TEST PROCEDURE

A vehicle test procedure has been developed to characterize the vehicle level thermal impact of solar reflective glazings. The U.S. Department of Energy's National Renewable Energy Laboratory (NREL) uses outdoor testing to determine the behavior of SRF under actual solar environmental conditions. Two vehicles are used in a test program; one vehicle is left with the production glazings and the other vehicle's glazings are modified. The advantage of using two vehicles is that the impact of day to day environmental differences are minimized. Additionally, comparing a temperature difference between the baseline and test vehicles using the same data system reduces the impact of systematic errors. Theoretically, the same systematic error is incurred by both measurements and cancels out when the temperatures are subtracted.

A two day test sequence is utilized for each glazing configuration. As shown in Figure 1, Day 1 consists of a soak test where the peak soak temperatures of the baseline and test vehicle are measured. After the peak temperatures are attained, a cooldown test is performed. The vehicles are operated at idle with the air conditioner operating at maximum fan speed and 100% recirculation air. On Day 2, a coheat test is performed. We measured the power of a ceramic heater required to maintain the cabin interior air temperature at a constant level, eliminating the effect of the thermal capacitance of the vehicle interior. As the solar gain increases, the heater power decreases. The difference in heater power between the baseline vehicle and the test vehicle is the solar power reflected by the SRF.

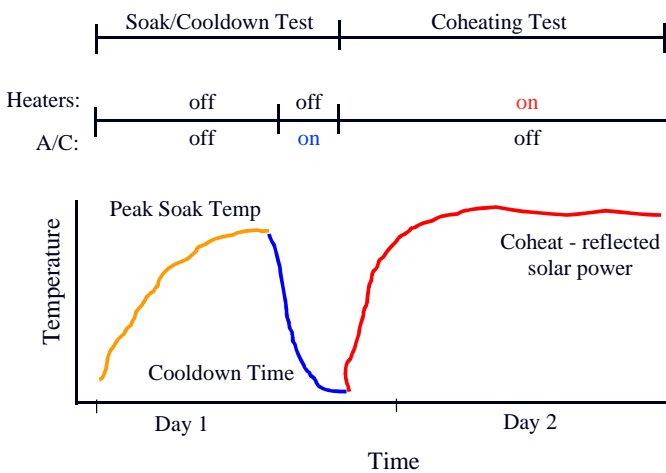


Figure 1 Vehicle Test Procedure

Prior to testing the SRF, both vehicles are tested with their production glazings to characterize any differences between the vehicles. In addition to the soak, cooldown, and coheat tests as described above, a tracer gas decay test to determine the air leakage is also performed.

VEHICLE TEST RESULTS

Two separate vehicle test programs were performed to determine the impact of SRF. From September to November 1999, two minivans were tested in Golden, CO. and Phoenix, AZ. A pair of SUVs were tested from June to October 2000.

MINIVAN – Although both minivans had a champagne pearl exterior and camel interior, one was a model year 1998 and the other was a 1999. The vehicles were oriented facing south in a front-back configuration. The baseline vehicle was the more southward vehicle and defined as Vehicle A. Correspondingly, the SRF test vehicle was the more northward vehicle and defined as Vehicle B. Thermocouples were located at the passenger breath, rear left breath, and driver foot. Surface thermocouples were located on the instrument panel (IP), windshield interior, driver sidelite, and left rear privacy sidelite.

During the soak test, the vehicles were in the 100% recirculation mode. The baseline soak test revealed that, despite the different model years, the vehicles were approximately thermally equivalent with the IP, breath, and windshield thermocouples within 0.5°C (1°F). Figure 2 shows the rear head temperature for the two vehicles were very similar.

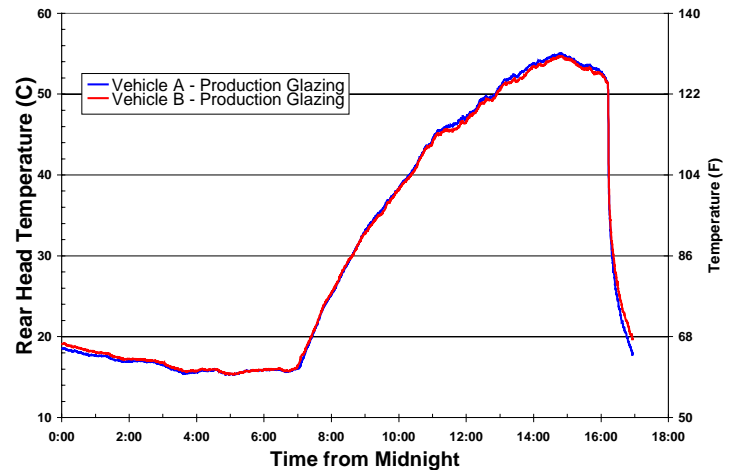


Figure 2. Rear Breath Temperature, Baseline, Phoenix, 10/20/99

The baseline cooldown test revealed that Vehicle B took a longer time to cool to 25°C (77°F). The baseline coheat test identified a difference in heater power required to maintain the vehicles at the same constant temperature. With these biases identified, comparative data during the SRF tests were adjusted accordingly to eliminate generic vehicle to vehicle differences.

Two glazing configurations were tested in Vehicle B.

- All glazings with 3M SRF
- Windshield only with 3M SRF

The 3M SRF applied to all glazings reduced the average breath temperature by 4.6°C (8.3°F) while the SRF windshield reduced the average breath temperature by 2.5°C (4.5°F). Table 2 shows the IP and windshield were also cooler when SRF was applied to the vehicle glazings.

Table 2. Reduction in maximum temperature

Glazing Configuration	Average Breath Temp °C (°F)	IP Temp °C (°F)	Windshield Temp °C (°F)
SRF all glazings	4.6 (8.3)	6.3 (11.3)	9.5 (17.1)
SRF windshield	2.5 (4.5)	4.7 (8.5)	8.7 (15.7)

The coheat test determined the 3M SRF on all glazings reflected an average of 486 W of solar power between 10:00 and 14:00 and the SRF windshield alone reflected 348 W.

Analysis predicted that the highest solar gain for a minivan in Phoenix in November was predicted to occur when the vehicles were oriented in the southwest direction. With the test vehicle configured with SRF on all glazings, the vehicles were rotated to the southwest and the coheat test measured the average reflected power increase to 534 W.

The SRF resulted in lower initial temperatures and lower solar loads during the stationary cooldown test. For the vehicle with SRF installed on all glazings, the time to 25°C (77°F) was reduced by 3.75 minutes. This means the air-conditioning system could operate at a reduced energy level with SRF installed and provide the same comfort level. Since the average time to 25°C (77°F) was approximately 20 minutes, the air-conditioning compressor would require roughly 19% less power to reach 25°C (77°F) with SRF applied to all the windows. Since the ambient temperature of the test day impacts the time to 25°C, the predicted reduction in air-conditioning compressor power is an estimate.

SUV – Two SUVs were tested to determine the impact of SRF. The testing was conducted primarily at DSET Laboratories in Phoenix, AZ. The vehicles, which had sequential VINs, black exteriors, graphite interiors, leather seats, and were oriented facing south in a front-back configuration. The vehicles were fully instrumented including heat flux gauges between the headliner and roof. During the soak test, the HVAC systems were in

0% recirculation mode which allowed the passenger compartments to breath through the HVAC systems.

The testing methods described in the vehicle test procedure section of this paper were applied to the SUVs. A series of baseline tests were performed to understand and characterize the difference between the vehicles. Vehicle B was hotter at most locations in all of the baseline tests. Figure 3 shows the average breath (four locations) temperature for two of the baseline tests. Reviewing the data from the four baseline tests, the maximum breath temperature for Vehicle B was 0.7°C (1.5°F) hotter than Vehicle A. Therefore, the maximum breath temperatures in Vehicle B in all subsequent tests were reduced by this amount to account for the vehicle differences.

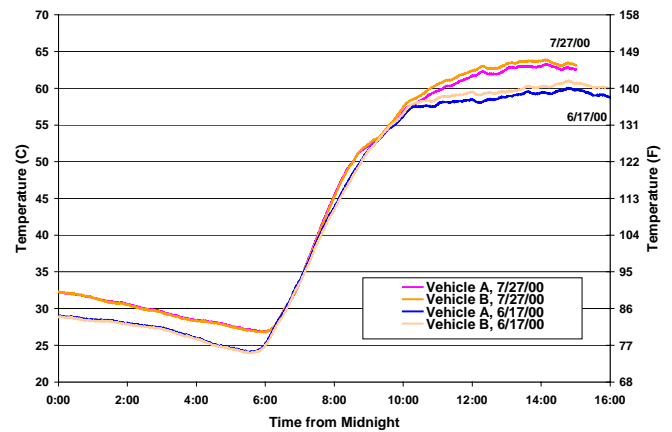


Figure 3. Average Breath Temperatures, Baseline

Figure 4 shows the driver sidelite interior temperature peaks early in the day with the morning solar load. The left rear privacy glass interior temperature also peaks early, but at a significantly higher temperature due to the higher absorptivity. The higher glazing temperature would add to the thermal discomfort of a person sitting in the rear seats at startup. As the vehicle speed increases, the increased heat transfer to the exterior will reduce the privacy glass temperature. The windshield, with a lower absorptivity than the privacy glass, peaks at a lower temperature and later in the day when the solar load favors the front of the south facing vehicle.

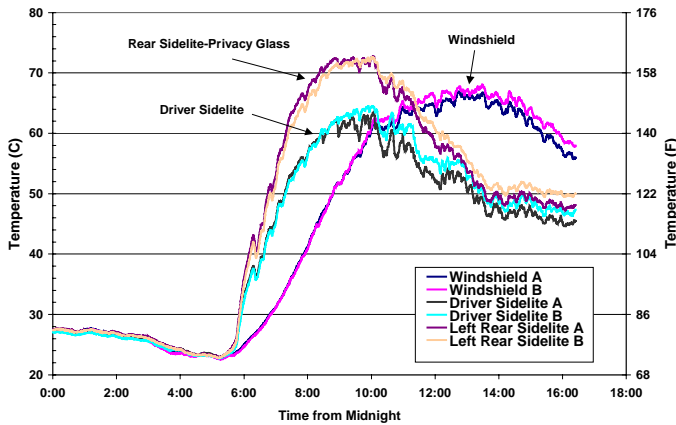


Figure 4. Surface Temperatures, Baseline, 6/17/00

The maximum breath temperature recorded was 65.5°C (150°F) and the maximum ambient temperature was 46.1°C (115°F). At the IP and exterior vehicle skin, the maximum temperatures were 88.9°C (192°F) and 87.8°C (190°F), respectively.

Repeatability problems were experienced during the baseline coheat testing; therefore, the test was not run on all the glazing configurations. The coheat data were used to calculate some of the heat transfer parameters in the passenger compartment thermal model.

The cooldown performance of Vehicle A was erratic, which resulted in a slower cooldown compared to Vehicle B. Using the time for the breath temperature to attain 30°C as a comparison parameter, there was no clear bias identified. This was due to day to day ambient temperature variations. In tests with high ambient temperatures, the average breath temperature did not attain 30°C. A passenger compartment thermal model was developed to assess the impact of the SRF on air-conditioning compressor size.

In the comparative phase of the testing, four glazing configurations were tested in Vehicle B.

- All glazings with 3M SRF
- 3M SRF windshield and four sidelites
- 3M SRF windshield and two sidelites
- 3M SRF windshield

Figure 5 shows the reduction in breath and IP temperatures due to the SRF. The configuration with SRF on all glazings had the best thermal performance with a 1.8°C (3.2°F) reduction in maximum breath temperature. The maximum IP temperature was reduced by 3.4°C (6.1°F) in this case. The reduction in breath temperature for the other configurations is shown in Figure 6. Possible explanations for the smaller thermal impact of the SRF compared to what was measured during the minivan testing include reduced window area, different windshield angles, and time of the year the testing was performed.

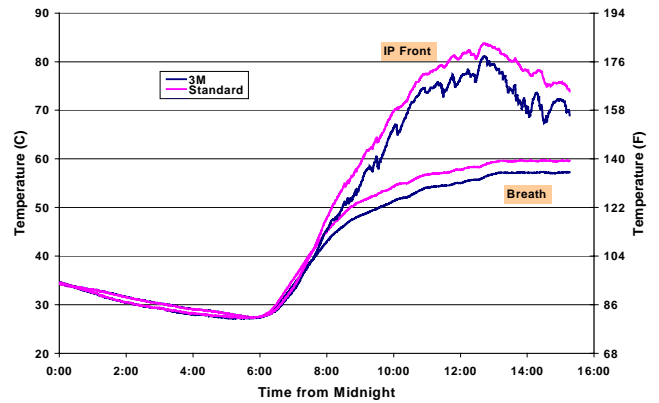


Figure 5. SRF all glazings, Soak Test, 7/21/00, Black SUV

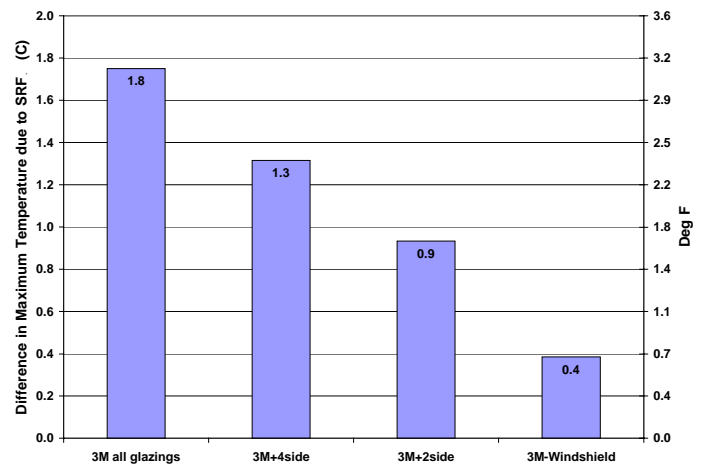


Figure 6. Reduction in Maximum Breath Temperature

Two additional tests were performed to gather data to compare with the performance of the SRF. In the first test, all of the glazings in Vehicle B were covered with foil simulating a high performance heat rejecting glazing system. As expected, there was a significant reduction in all temperatures. Figure 7 shows the breath temperatures and ambient temperature. The breath temperature was still 10°C (18°F) above ambient when all the transmitted solar energy was blocked. The heat gain from other surfaces demonstrate that reducing the peak soak temperature is not just a glazing issue, it is a vehicle system issue.

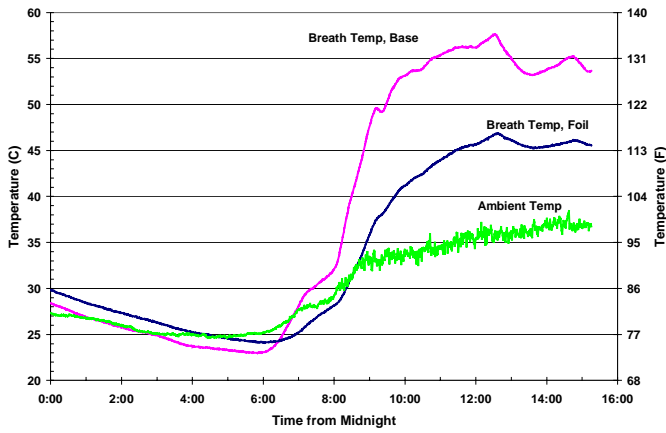


Figure 7. Foil on all Glazings, 8/25/00

In a second test, foil was applied to the roof of Vehicle B to simulate a light colored exterior. The glazings in both vehicles were production glass. The maximum breath temperature was reduced by 2.1°C (3.8°F). This was similar to the thermal impact of SRF on all glazings. Figure 8 shows the heat flux through the roof. Vehicle A experiences heat gain through the roof throughout the day while the foil roof vehicle had heat loss through the roof. With a light colored vehicle and production glass, the roof is a heat loss mechanism and increasing roof insulation would actually cause the passenger compartment to be hotter. Again these data illustrated reducing the peak soak temperature is a system challenge that requires a system solution

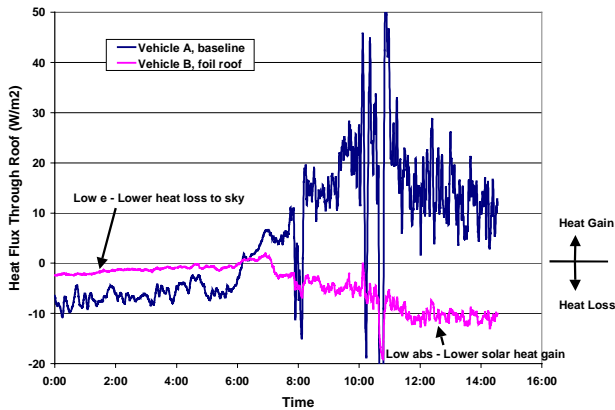


Figure 8. Heat Flux, Foil on the Roof of Vehicle B

VEHICLE MODELING

PASSENGER COMPARTMENT THERMAL MODEL - Since the SUV cooldown tests did not yield consistent results, a first order cooldown model of the passenger compartment was developed to allow an assessment of the air-conditioner compressor size with and without SRF.

The interior mass of the passenger compartment was defined as a single node with a heat loss path to ambient. Figure 9 shows the solar heat gain from all

surfaces (Q_{solar}) and heat loss due to the operation of the air conditioner (Q_{evap}).

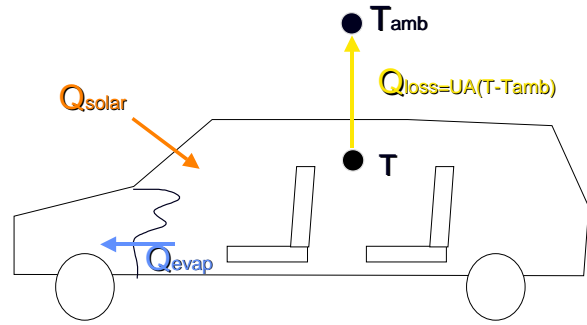


Figure 9. Passenger compartment Thermal Model

Equation 1 results from performing a heat balance calculation on the passenger compartment and integrating.

$$T = T_{amb}^* + \left(T_{init} + T_{amb}^* \right) e^{-\left(\frac{UA(t)}{mc_p} \right)} \quad (1)$$

where

$$T_{amb}^* = \frac{Q_{solar}}{UA} + \frac{Q_{evap}}{UA} + T_{amb} \quad (2)$$

Vehicle B air-conditioning performance data were used to define the parameters because these data were more consistent than Vehicle A. The overall heat transfer coefficient (UA) was determined from night coheat test data. An assumption is that the overall heat transfer coefficient at night equals the overall heat transfer coefficient during the day. Steady state thermal conditions were assumed just prior to the start of cooldown to allow the calculation of Q_{solar} . It was also assumed that Q_{evap} and Q_{solar} remained constant throughout the cooldown. Since test data were used to define the parameters, this model is specific for a black SUV tested in Phoenix in the summer.

Figure 10 illustrates the good correlation between the model and test breath temperature. After 30 minutes, the breath temperature is approximately 31°C (88°F). When the initial temperature is reduced by 1.8°C (3.2°F) and the Q_{solar} is reduced by 182 W simulating incorporation of SRF on all glazings, the breath temperature is reduced at every time point. By reducing the amount of thermal energy removed by the air-conditioning system by 6.5%, the breath temperature at 30 minutes is increased back to 31°C (88°F). This

means that incorporating SRF allows a reduction in air-conditioning power without degrading the thermal cooldown performance of the passenger compartment. Figure 11 was generated by performing this analytical procedure with different initial temperatures. The perfect reflective window system (foil) resulted in a 40% reduction in A/C power. The curve does not extend to 100% because the vehicle can not be initially cooler than the ambient temperature which is warmer than the 31°C (88°F) at 30 minutes criteria; therefore, some air conditioning will be needed.

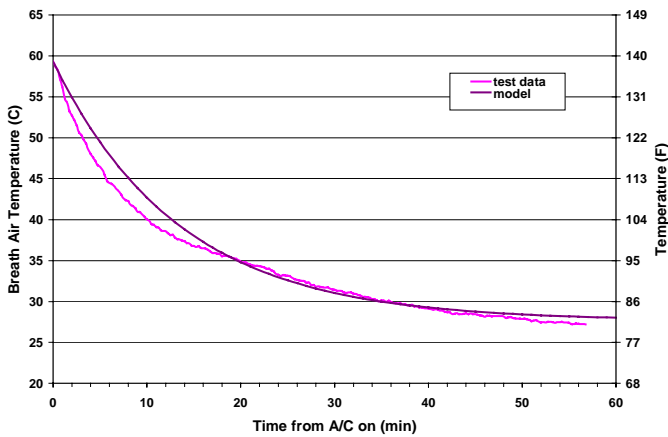


Figure 10. Vehicle B Breath Air Temperature - Cooldown Model

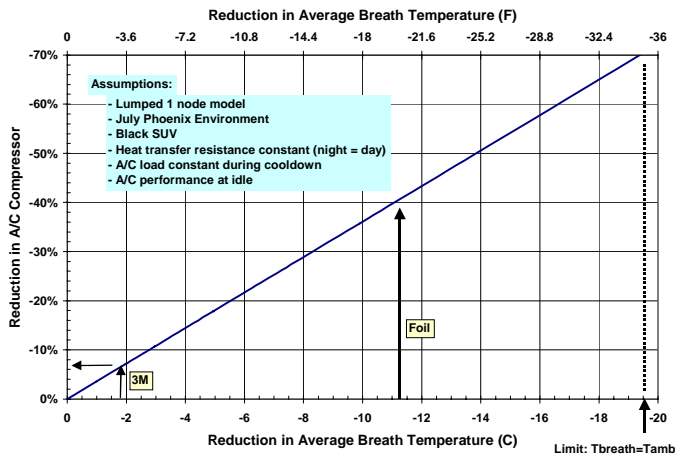


Figure 11. Reduction in Air-Conditioner Compressor Size

ADVISOR - After the reduction in air-conditioning compressor size was estimated, the fuel use was modeled using the simulation tool ADVISOR. NREL's ADvanced Vehicle Simulator^{5,6} is designed for quick analysis of the performance and fuel economy of conventional, electric, and hybrid vehicles. ADVISOR

can be used to model vehicle efficiencies, to assess impacts of applying innovative technologies to vehicle configurations, to develop novel energy management strategies, and to integrate simulated and real-life assessments.

The impact of the reduced air-conditioning system was estimated for an SUV driven over the SCO3 drive cycle. NREL was provided with details of the engine, transmission, and vehicle geometry and these data were used to generate an ADVISOR model. Initial simulations over the UDDS and HWFET drive cycles showed the transmission and auxiliary losses were low and the fuel economy was high. After a small adjustment to the loss coefficients, the fuel economy for the city (UDDS) matched to within 0.05% and highway (HWFET) matched to within 0.5%.

The air-conditioning load of 4000 W was then added to the baseline auxiliary load of 1000 W and the vehicle operation was simulated over the SCO3 drive cycle. This was defined as the baseline vehicle simulation from which the % differences were calculated. Then the air-conditioning load was reduced incrementally and Figure 12 was generated. Assuming a 6.5% decrease in air-conditioning power due to SRF, the fuel economy is increased 1.3% or approximately 0.2 mpg. Figure 13 shows the reduction in NO_x of 2.5%. Since Figures 12 and 13 are not directly related to SRF, they can be used to assess the impact of a reduction in the air-conditioning compressor regardless of the method used to reduce the peak soak temperature.

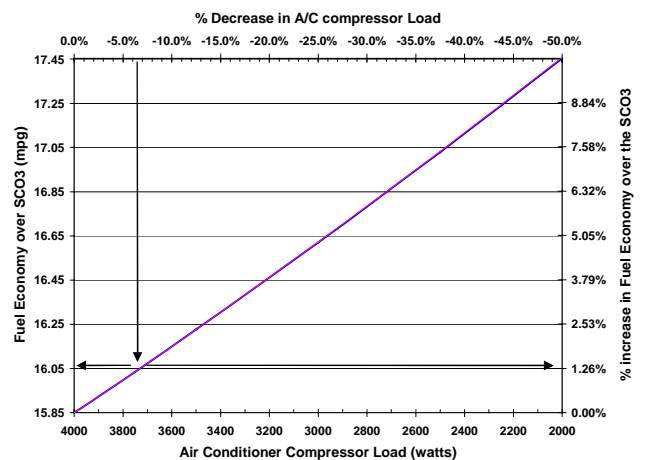


Figure 12. Impact of SRF on Fuel Economy for an SUV

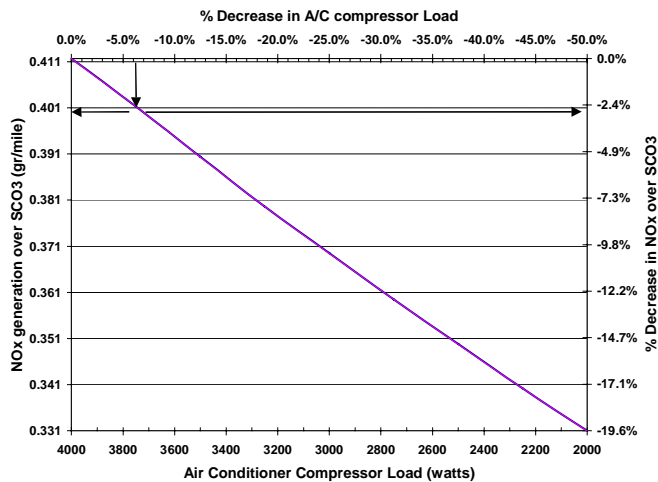


Figure 13. Impact of SRF on NO_x generation for an SUV

CONCLUSION

With the development of high fuel economy vehicles and hybrid electric vehicles, the energy consumed by the air-conditioning system will become increasingly important. With the large number of vehicles in this country, the energy consumed by the air conditioning in all vehicles is significant. The goal at NREL's Center for Transportation Technologies and Systems is to work with industry to reduce the amount of fuel used for climate control. With the large number of vehicles sold each year, a small change in today's vehicles can make a large impact on national fuel consumption.

Decreasing the peak soak temperature enables the air-conditioner system size to be reduced, the fuel economy to be increased, and the tailpipe emissions to be reduced. SRF is one way to reduce the peak soak temperature. The tests on the minivans and SUVs demonstrated the thermal impact of SRF. The corresponding fuel economy and tailpipe emissions were predicted over the SC03 drive cycle using ADVISOR. SRF is an important part of the system solution to minimize the peak soak temperature.

ACKNOWLEDGMENTS

This work was supported by DOE's Hybrid Vehicle Propulsion Program, which is managed by the Office of Advanced Transportation Technologies. The authors appreciate the support of Robert Kost and Roland Gravel, DOE Program Managers; Terry Penney, NREL's HEV Technology Manager; and Barbara Goodman, Director of the Center for Transportation Technologies and Systems. The authors would like to acknowledge the significant contributions provided by industry and by our colleagues at NREL. Our industry partners in this project

provided significant hardware and feedback. 3M provided glazing systems and technical support. In addition, we recognize the significant contribution of Tom Thoensen, who assisted with the construction and operation of the experiments. Valerie Johnson assisted with the ADVISOR analysis and Bill Marion helped with determining the worst-case vehicle orientation. Stephanie Saxby of 3M helped with the experimental design and statistical analysis.

REFERENCES

1. Farrington, R.; and Rugh, J.; October 2000, "Impact of Vehicle Air Conditioning on Fuel economy, Tailpipe Emissions, and Electric Vehicle Range." NREL Report No. CP-540-28960, Golden, CO: NREL
2. Federal Register, October 22, 1996. "Part II Environmental Protection Agency. Motor Vehicle Emissions Federal Test Procedure Revisions: Final Regulations." 40 CFR Part 86
3. Clean Air Vehicle Technology Center; October 1999. "Effect of Air-conditioning on Regulated Emissions for In-Use Vehicles, Phase I, Final Report." Prepared for Coordinating Research Council, Inc. CRC Project E-37. Also available at <http://www.crao.com>
4. Farrington, R.; Cuddy, M.; Keyser, M.; and Rugh, J.; 1999, "Opportunities to Reduce Air-conditioning Loads through Lower Cabin Soak Temperatures." NREL Report No. CP-540-26615, Golden, CO: NREL
5. Wipke, K.; Cuddy, M.; Burch, S.; 1999. "ADVISOR 2.1: A User-Friendly Advanced Powertrain Simulation Using a Combined Backward/Forward Approach." 14 pp.; NREL Report No. JA-540-26839, Golden, CO: NREL
6. Wipke, K.; Cuddy, M.; Bharathan, D.; Burch, S.; Johnson, V.; Markel, A.; and Sprik, S. 1999. ADVISOR 2.0: A Second-Generation Advanced Vehicle Simulator for Systems Analysis. 14 pp.; NREL Report No. TP-540-25928, Golden, CO: NREL

CONTACT

<http://www.nrel.gov>
<http://www.ott.doe.gov/coolcar>
 rob_farrington@nrel.gov
 john_rugh@nrel.gov
 jaboettcher@mmm.com